



APPLICATION OF LASER-GENERATED ULTRASOUND TO EVALUATE WALL THINNED PIPE

Bong-Min Song¹, Jin-Hyun Kim¹ and Joon-Hyun Lee¹

1. School of Mechanical Engineering, Pusan National University, Busan 609-735, Korea

ABSTRACT

The objective of this study is the development of non-contacting technique to evaluate the size of wall-thinned defect using laser-generated guided waves. Therefore, while the conventional studies on guided waves were focused on the long-range inspection for the presence of the defect, this study deals with the local inspection of the area where the defect is apt to generate for a closer defect sizing. For this aim, the non-contacting system of laser with linear slit array and air-coupled transducer was used in order to generate and detect guided waves and carbon steel pipe with elliptical defects which is similar to actual corrosion was adopted as a specimen. As a result, the characteristics of guided waves with varying shape of wall-thinned defect in carbon steel pipe are investigated and consequently the trends of these characteristics are analyzed for evaluating defect sizing quantitatively.

Keywords: wall-thinning, Laser-generated guided wave, Air-coupled transducer, linear slit array

1. INTRODUCTION

Wall thinning of carbon steel pipe is mainly caused by FAC(Flow-Accelerated Corrosion) in secondary pipe system of nuclear power plant^[1]. In order to evaluate this material degradation, scanning technique is being used by point by point inspection method. Because there are a lot of pipes and they have very complicated network, this point by point inspection method is time consuming process with high cost. And this method usually uses bulk wave with contact method, there is difficulty for inspection of pipes at high temperature. Therefore, techniques using guided wave with non-contact method such as EMAT, MsS, air-coupled transducer and laser-ulasonics are necessary to overcome these problems^[2]. Among these techniques, EMAT and MsS launch ultrasound in low frequency range to inspect long range area. These techniques are not appropriate to inspect small cracks or corroded part due to their long wave length. Otherwise, laser-ulasonics has a large

progressive improvement for the generation of guided wave with narrow band frequency using slit mask. Slit mask improves the directivity and makes selective mode generation available by adjusting the interval between arrays^[3]. In addition, air-coupled transducer for detection of guided wave has high sensitivity and reception of specific mode of guided wave is possible by slanting its receiving angle to a leak direction of selected mode. A hybrid system of laser generation and air-coupled detection was adopted to utilize these advantages in this study.

2. SPECIMEN AND EXPERIMENTAL SETUP

The specimens used in the tests are 6mm thick carbon steel pipes. To evaluate the guided wave interaction with defect of varying depth in pipes, elliptical defect of a constant width 48mm and varying depth 1.2, 2.4 or 3.6 mm was machined on the inner surface of 6mm thick pipe having diameter of 114.3mm. Figure 1 shows the shape of the above mentioned defect on carbon steel pipe.

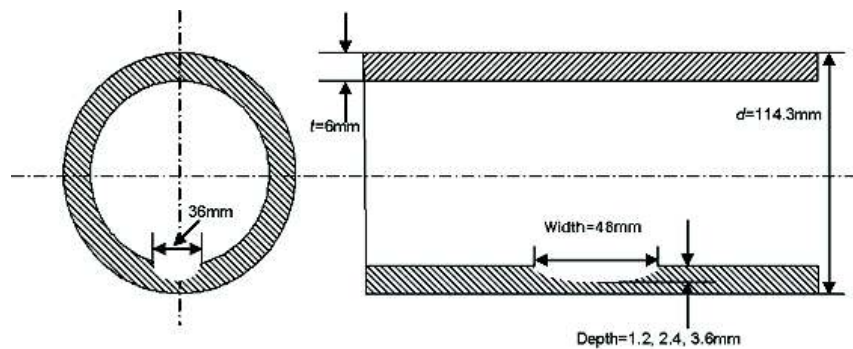


Figure 1 Shape of wall-thinned defect on carbon steel pipe

A schematic diagram of the apparatus used to perform experiment is shown in Figure 2. As shown in this figure, the laser and air-coupled transducer are positioned on the same side of the test pipes and act as the generator and detector of the guided wave signals, respectively. A wavelength of fiberized Nd:YAG pulse laser system used to generate ultrasonic waves is 532 nm and this pulse laser system emits energy of 32 mJ at one pulse. The beam of this laser illuminates a linear array slit and transmitted beam act as line source on the pipe. The guided wave generated by this source propagates distance of 90 mm from the source to the receiver, perpendicular to the surface of the pipe, and is subsequently detected using the air coupled transducer with the a standoff of 15 mm from the outer surface of plate. In addition, the received signals from the air-coupled transducer are magnified by the amplifier and displayed through the signal averaging scheme with 1000 sampling data on the screen of oscilloscope.

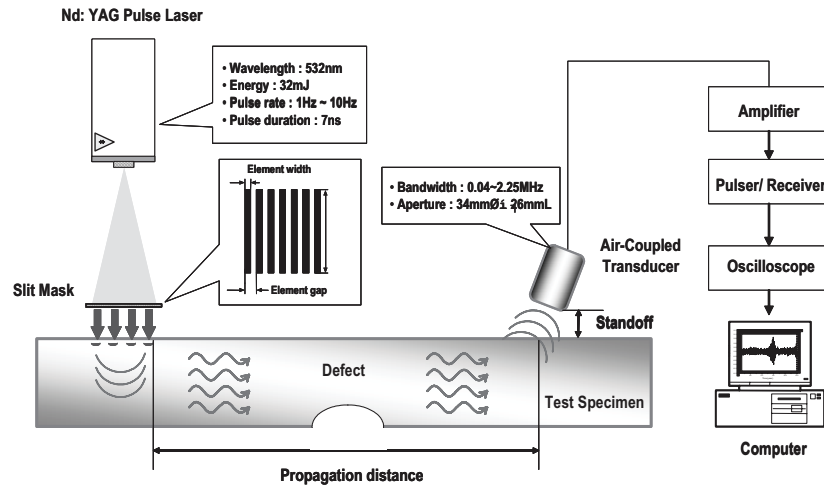


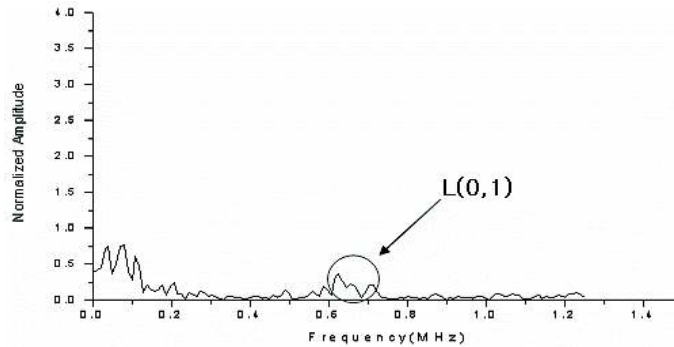
Figure 2 Schematic diagram of experimental setup

3. NUMERICAL SIMULATION

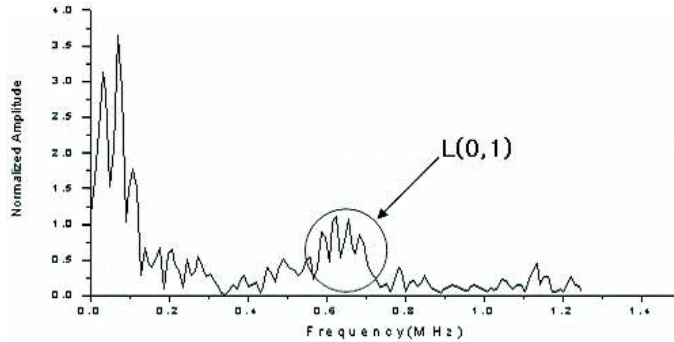
Simulation of laser generated ultrasound are carried out to show the validity before experiment. For simulation of laser generated ultrasound, modeling technique used is sequentially coupled thermal-mechanical analysis^[4]. Because when laser illuminates on the surface of material, the heat spot makes thermo-elastic region. Figure 3 shows frequency spectrum of simulation result. This result represents the fact that amplitude of signal around 0.65 MHz is higher than other frequency range except low frequency range under 0.2 MHz. This frequency range is the same as L(0,1) mode of guide wave in this condition. All simulations are performed using the commercial finite element analysis code ABAQUS 6.5.

Table 1 Material Coefficient of Carbon Steel Pipe

Density [kg/mm ³]	Young's Modulus [GPa]	Thermal Conductivity [J/mS]	Thermal Expansion Coefficient [/]	Specific Heat [J/kg□]
7.872 x 10 ⁻⁶	80	36	17 x 10 ⁻⁶	504 x 10 ⁻³



(a) Defect free



(b) 1.2mm wall-thinning

Figure 3 Frequency Spectrum of Laser Generated Ultrasound

4. SELECTIVE GENERATION AND RECEPTION OF GUIDED WAVE MODES

Guided waves are dispersive and these features make not only the generation of a single mode but also selective generation of desired mode difficult. Therefore, many techniques about the generation of guided waves have been developed. Among these methods, this study used a linear slit array which can generate the specific mode selectively. When an illuminated laser beam transmits the slit, the signal with the wavelength which correspond to the element gap of slit array (Δs) is generated on the surface of the object. Here, the relation among the wavelength, phase velocity and frequency of generated signal is as shown in equation 1. Figure 4 represents the process to generate the desired mode using this relation. As shown in Figure 4, the diagonal line with a slope of $\Delta s/d$ is described in dispersion curves and crossings are generated between the diagonal line and the dispersion curves. Therefore, various modes with different frequency are generated simultaneously.

$$C_{ph} = f \cdot \lambda = f \cdot \Delta s = f \cdot d \cdot \left(\frac{\Delta s}{d} \right) \quad (1)$$

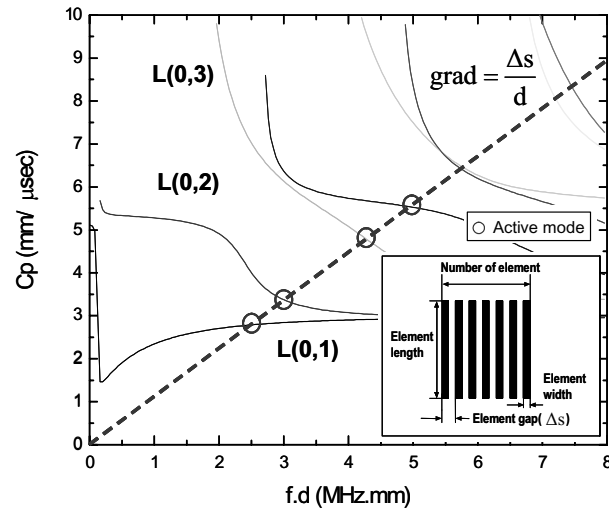


Figure 4 Determination of desired modes using the relation between slit gap and the wavelength of generated signal in phase velocity dispersion curve

The modes generated by laser and linear slit array are received selectively by air-coupled transducer with the bandwidth of 0.04~2.25MHz. Here, it is important to control the angle of air-coupled transducer since the received signal can be changed considerably by the slight turning of air-coupled transducer. Such a receiving angle of air-coupled transducer is determined in terms of the phase velocity of the desired mode and the wave velocity of the air, based on the following Snell's law as shown in Equation 2^[5].

$$\sin \theta = \frac{C_{air}}{C_{ph}} \quad (2)$$

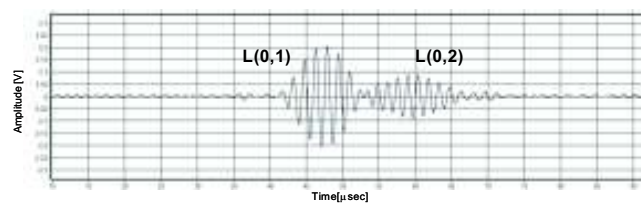
Where θ is the angle for receiving a specific mode and represents the velocity of the propagating wave in air. In this study, is 340 m/s and the phase velocity is obtained from the cross points shown in Figure 4. Here, the interval between slits, the width and the number of slits are fabricated 4.5 mm, 2.25 mm and 7 respectively. Table 2 shows frequency, phase velocity, receiving angle of the modes obtained from theoretical phase velocity dispersion curves for each specimen.

Table 2 Theoretical values of the modes obtained from the dispersion curves

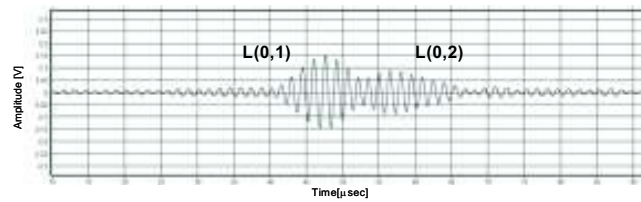
Element gap [mm]	Mode	Frequency [MHz]	Phase velocity [mm/μsec]	Receiving angle [degree]
4.5	L(0,1)	0.64	2.89	6.4
	L(0,2)	0.68	3.06	6

5. EXPERIMENTAL RESULT

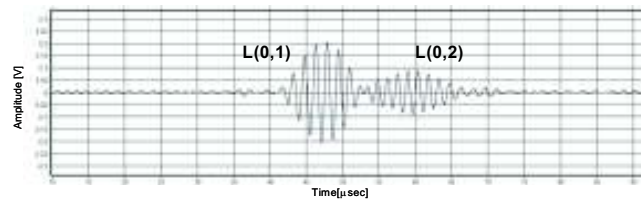
Figures 5(a)-(d) show the response of the pipe 90mm from the laser source received by air-coupled transducer with the receiving angle of 6.4 degree after interaction without defect and with 1.2-, 2.4- and 3.6mm-deep elliptical defects respectively, which were located 20mm from the source. The signals of Figures 5(a)-(d) include both L(0,1) with 0.64MHz and L(0,2) with 0.68MHz. However, according to deeper defect, the magnitude of L(0,2) is decreased while that of L(0,1) is nearly constant.



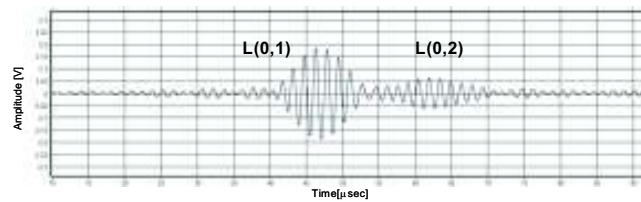
(a) without defect



(b) with 1.2mm deep defect



(c) with 2.4mm deep defect



(d) with 3.6mm deep defect

Figure 5 Signal with elliptical defect on 6mm-thick pipe according to the variation of reduced thickness

This fact demonstrated in time-frequency analysis of Figures 6(a)-(d). As shown in Figures 6(a)-(d), L(0,1) with the frequency of 0.64 MHz and L(0,2) with that of 0.68 MHz emerge concurrently at no defect, and then the magnitude of L(0,2) becomes smaller continuously by its disappearance. The normalized ratio of the amplitude of L(0,1) divided by that of L(0,2) in Figure 7 is proportional to defect depth.

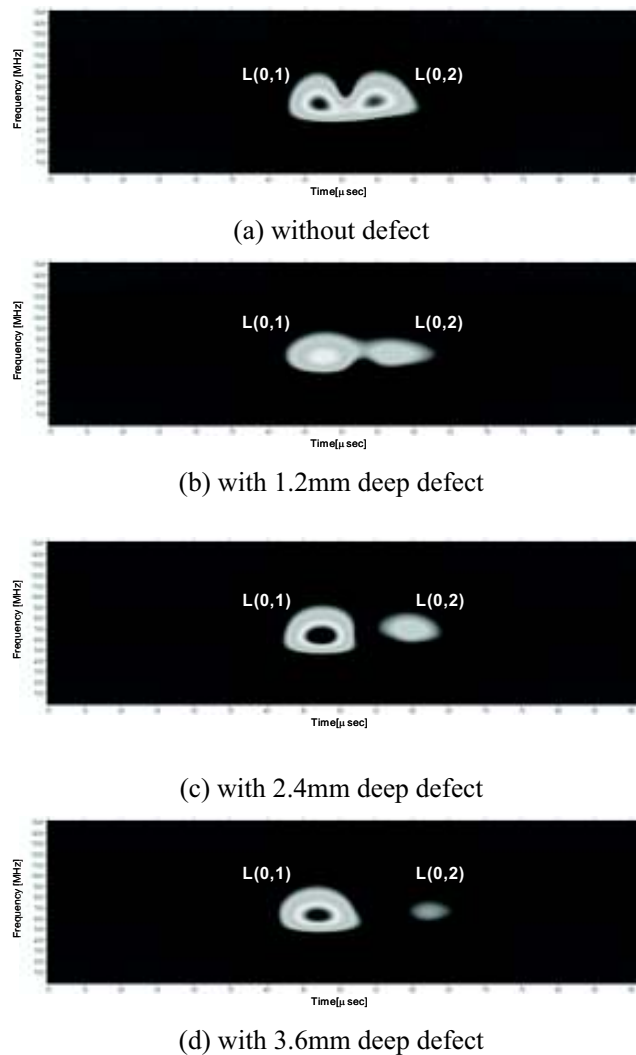


Figure 6 Time-frequency analysis for signal with elliptical defect on 6mm thick pipe according to deeper defect

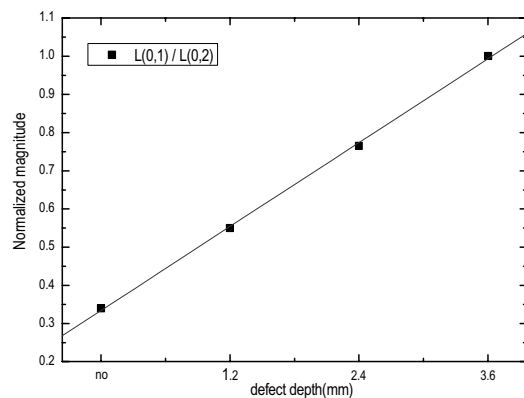


Figure 7 Normalized ratio of L(0,1) to L(0,2) mode versus elliptical defect depth

6. CONCLUSIONS

Result of numerical simulation shows similar frequency characteristic with experimental result. In pipes, defect depth was proportional to the normalized ratio of the magnitude of L(0,1) divided by that of L(0,2). In addition, the effect of defect width on pipes was the variation of the magnitude of L(0,1) and L(0,2). The above-mentioned results indicate the possibility of evaluating quantitative defect sizing in pipes. However, they have the problem that it is difficult to distinguish the shape of defect accurately due to the similar directivity of variation. Therefore, to solve this problem, studies for more cases must be carried out and then more detail rule for evaluation defects being established. In this aspect, it is considered that the present study can act as the fundamental concept.

7. ACKNOWLEDGEMENT

This work was supported by the Ministry of Science & Technology through Basic Atomic Energy Research Institute (BAERI) program.

8. REFERENCE

- 1) R.B. Dooley, V.K. Chexal : Flow-accelerated corrosion of pressure vessels in fossil plants, *International Journal of Pressure Vessels and Piping*, 77: 85-90, 2000.
- 2) Robert E. Green Jr. : Non-contact ultrasonic techniques, *Ultrasonics*, 42: 9-16, 2004.

- 3) Hongjoon Kim, Kyongyoung Jhang, Minjea Shin and Jaeyeol Kime : A Noncontact NDE Method Using a Laser Generated Focused-Lamb Wave with Enhanced Defect-Detection Ability and Spatial Resolution, *NDT&E International*, 39:312-319, 2006.
- 4) Adele L'Etang, Zhihong Huang, FE Simulation of Laser Generated Surface Acoustic Wave Propagation in skin, *Ultrasonics*, 44: e1243-e1247, 2006.
- 5) Kim HM, Lee TH and Jhang KY. : Non-Contact Guided Wave Technique with Enhanced Mode-Selectivity, *J Korean Soc NDT*, 24(6):597-602, 2004.
- 6) M.Z. Silva, R. Gouyon, F. Lepoutre : Hidden Corrosion Detection in Aircraft Aluminum Structures Using Laser Ultrasonics and Wavelet Transform Signal Analysis, *Ultrasonics*, 41: 301-305, 2003.
- 7) A.S. Murfin and R.J. Dewhurst : Estimation of Wall Thinning in Mild Steel Using Laser Ultrasound Lamb Waves and A Non-steady-state Photo-emf Detector, *Ultrasonics*, 40: 777-781, 2002.
- 8) R. B. Thompson : Physical Principles of Measurements with EMAT Transducer, *in Physical Acoustics-Principles and Methods*, 19: 157-199, 1990.
- 9) David A. Hutchins, William M. D. Wright and Gordon Hayward : Air-Coupled Piezoelectric Detection of Laser-Generated Ultrasound, *IEEE Trans. Ultrason. Ferroelec. Freq. Contr.*, 41A(6): 796-805, 1994.
- 10) R.D. Huber, R.E. Green Jr. : Noncontact Acousto-ultrasonics Using Laser Generation and Laser Interferometric Detection, *Material Evaluation*, 49 : 613-618, 1991.

IVrd NDT in PROGRESS
